

Fractal Modeling of Mammogram and Enhancement of Microcalcifications

H. Li^{1,2}, K. J. R. Liu¹, and S. C. B. Lo²

¹Electrical Engineering Department and Institute for Systems Research
University of Maryland at College Park, College Park, Maryland 20742

²ISIS Center, Georgetown University Medical Center, Washington, D.C. 20007 *

Abstract

According to the theory of deterministic fractal geometry, images can be modeled by deterministic fractal objects which are attractors of sets of two dimensional affine transformations. In this paper, a fractal modeling approach is developed to analyze and model mammographic breast tissue background. We show that general mammographic parenchymal and ductal patterns can be well modeled by a set of parameters of affine transformations. Therefore, microcalcifications can be enhanced by taking the difference between the original image and the modeled image. Our results are compared with those of the partial wavelet reconstruction and morphological operation approaches. The evaluation results demonstrate that the fractal modeling method is an effective way to enhance microcalcifications, and thereby may facilitate the radiologists' diagnosis. It may also be able to improve the detection of microcalcifications in a computer system.

I. INTRODUCTION

The task of detection of microcalcifications for the diagnosis of breast cancer is a difficult one. Dense breasts, improper technical factors or simple oversight by radiologists may contribute to the failure of detecting microcalcifications [1]. Especially, some subtle case, such as faint microcalcifications which have small sizes and are superimposed on dense breast regions, are very difficult to detect, even for experienced radiologists. Consequently, computer-assisted detection of microcalcifications has aroused a great deal of interest. Microcalcification enhancement is a important step in any computer-assisted systems. In this study, we propose a novel enhancement technique. Our basic idea is that if we can tell the different properties of disease patterns (such as microcalcifications) and background patterns in both spatial and frequency domains, then we can separate the whole image into different layers using different models according to the difference in patterns. One layer only contains disease pattern information. The other layer contains non-disease related background information. Hence, the disease pattern will be enhanced by taking the background layer from the original image.

Recently, both stochastic and deterministic fractal-based techniques have been applied in many areas of digital image processing, such as image segmentation and image analysis [2], [3]. Based on the deterministic fractal the-

ory, images can be modeled by deterministic fractal objects which are attractors of sets of two-dimensional affine transformations [4], [5], [6]. In this work, we use the deterministic fractal approach to model the mammographic background and to enhance microcalcifications. We observed that microcalcifications are visible as small objects which appear to be added to the mammographic background. Some of them are bright, some are faint. Microcalcifications can be characterized as different shapes. But compared with breast background tissue, they have less structure. On the other hand, the mammographic parenchymal and ductal patterns in mammograms possess structures with high local self-similarity which is the basic property of fractal objects. These tissue patterns can be constructed by fractal models, and be taken out from the original image, as such the microcalcification information will be enhanced. The results are very encouraging compared with those of partial wavelet reconstruction [7], [8] and morphological operation methods [9]. We anticipate that the proposed fractal approach is very helpful for radiologists to detect the microcalcifications, and also facilitates the evaluation procedures in a mammographic computer-aided diagnosis system.

II. THEORETICAL BACKGROUND

Given a complete metric space (\mathbf{X}, d) , we can define the metric space $(\mathcal{H}(\mathbf{X}), h)$, where $\mathcal{H}(\mathbf{X})$ is the space of compact subsets of \mathbf{X} , and the distance $h : \mathcal{H}(\mathbf{X}) \times \mathcal{H}(\mathbf{X}) \rightarrow \mathcal{R}$ between two sets A and B is the Hausdorff distance, which is characterized in terms of the metric d . Under these conditions, it can be shown that the metric space $\mathcal{H}(\mathbf{X})$ is complete according to the Hausdorff metric [4]. Let $f \in \mathcal{H}(\mathbf{X})$ be an original image to be modeled. We wish to find contractive affine map $\tau : \mathcal{H}(\mathbf{X}) \rightarrow \mathcal{H}(\mathbf{X})$, satisfying the requirement

$$\forall f_1, f_2 \in \mathcal{H}(\mathbf{X}), h(\tau(f_1), \tau(f_2)) \leq s \cdot h(f_1, f_2), \quad (1)$$

and such that

$$h(f, \tau(f)) < \delta, \quad (2)$$

where $s < 1$ and δ is a tolerance which can be set to different values according to different applications. The scalar s is called the contractivity of τ . τ can be a set of contractive mappings τ_i , i.e., $\tau = \cup_{i=1}^N \tau_i$. According to the deterministic fractal theory, a set of contractive mappings τ_i is the main part of an iterated function system (IFS). The definition of IFS is given as follows [4].

*This work was supported in part by an U.S. Army Grant DAMD17-93-J-3007 and an NSF NYI Award MIP-9457397.

Definition 1: An iterated function system (IFS) consists of a complete metric space (\mathbf{X}, d) with a finite set of contraction mappings $\tau_i : \mathbf{X} \rightarrow \mathbf{X}$, with respective contractivity factors s_i , for $i = 1, 2, \dots, N$, and its contractivity factor is $s = \max\{s_i : i = 1, 2, \dots, N\}$.

With the definition of IFS, one can state the important property of IFS in the following theorem.

Theorem 1: (The Collage Theorem) Let (\mathbf{X}, d) be a complete metric space. Let $L \in \mathcal{H}(\mathbf{X})$ be given, and let $\epsilon \geq 0$ be given. Choose an IFS $\{\mathbf{X}; \tau_i\}$ with contractivity factor $0 \leq s < 1$, so that

$$h(L, \cup_{n=0}^N \tau_n(L)) \leq \epsilon. \quad (3)$$

Then $h(L, A) \leq \epsilon/(1-s)$, for all $L \in \mathcal{H}(\mathbf{X})$, where A is the attractor of the IFS.

The proof of the Collage Theorem can be found in [4]. The Collage Theorem shows that, once an IFS is found, i.e., τ is known such that $h(f, \tau(f)) < \delta$ is satisfied, then from any given image f_0 and any positive integer n , one can get

$$h(f, \tau^{on}(f_0)) \leq \frac{1}{1-s} h(f, \tau(f)) + s^n h(f, f_0). \quad (4)$$

Since $s < 1$, we see that after a number of iterations, the constructed image $f_n = \tau^{on}(f_0)$ will be close visually to the original image f .

The key point of fractal modeling is to explore the self-similarity property of images. Real world images are seldom self-similar, so it is impossible to find a transformation τ for an entire image. But almost all real images have a local self-similarity. We can divide the image into n small blocks, and for each block find a corresponding τ_i . So finally, we can define $\tau = \cup_{i=1}^n \tau_i$.

III. ALGORITHM IMPLEMENTATION

Now we introduce a mathematical representation for digital gray-level images. Let $N_1 = [0, 1, \dots, M]$, $N_2 = [0, 1, \dots, N]$, $N_3 = [0, 1, \dots, L]$, respectively, then for any digital gray-level image $f(k, l)$, we have $(k, l, f(k, l)) \in N_1 \times N_2 \times N_3$. Let D_1, \dots, D_n and R_1, \dots, R_n be subsets of $N_1 \times N_2$, such that $\cup_{i=1}^n R_i = N_1 \times N_2$ and $R_i \cap R_j = \phi, i \neq j$. We call R_i the range squares, and D_i the domain squares. In practice, we can use mean square root metric and τ_i can be defined as

$$\tau_i(f(k, l)) = s_i \bar{f}(k, l)|_{(k, l) \in D_i} + o_i, \quad (5)$$

where

$$\bar{f}(k, l) = \frac{\sum_{i=0}^1 \sum_{j=0}^1 f(k+i, l+j)}{4}. \quad (6)$$

s_i is a scaling factor and o_i is an offset factor; they are blockwise constants on each R_i . The goal is: for each R_i ,

a $D_i \subset N_1 \times N_2$ and $\tau_i : N_1 \times N_2 \times N_3 \rightarrow N_3$ are sought such that

$$e_i = \sum_k \sum_l (f(k, l) - (s_i \bar{f}(k, l) + o_i))^2. \quad (7)$$

is minimized. Through solving $\frac{\partial e_i}{\partial s_i} = 0$ and $\frac{\partial e_i}{\partial o_i} = 0$, we get the optimal values of s_i and o_i . We put the optimal \hat{s}_i, \hat{o}_i into (7), and obtain the minimum error \hat{e}_i . Then, we set a uniform tolerance $\delta_i = \bar{\delta}$, and select the best D_i , such that $\hat{e}_i < \bar{\delta}$.

Suppose there is a cluster of microcalcifications or some single isolated ones on the image block above R_i , our intention is to find an area D_i on which the image has a similar structure as on R_i but does not have similar microcalcification patterns. Then when a difference between the original image and modeled image is taken, the microcalcifications will be enhanced. This means that when searching for D_i , the suitable D_i should not cover the region of R_i . In our algorithm, for each given R_i , we constrain the search way of D_i by $R_i \cap D_i = \phi$.

A. Fractal Modeling

The modeling process is summarized in the following algorithm:

Step 1: Initially, R_i are chosen to be nonoverlapping sub-squares of size 32×32 . A search is then performed for the domain squares which best minimized (7) and satisfied the constraint of D_i by $R_i \cap D_i = \phi$.

Step 2: If the value of (7) is less than a predetermined tolerance, then the corresponding D_i and τ_i are stored and the process is repeated for the next range square. If not, the range square is subdivided into four equal squares. This quadtreeing process was repeated until the tolerance condition was satisfied, or a range square of minimum size (here we set 8×8 pixels) is reached.

Step 3: The process is continued until the whole image is modeled. A choice of D_i , along with a corresponding s_i and o_i , determines the τ_i on R_i . Once all τ_i are found, we can define $\tau = \cup_{i=1}^n \tau_i$, such that $d(f, \tau(f)) < \delta$, where $\delta = n\bar{\delta}$, and n is the block number of R_i .

Step 4: Finally, based on the Collage Theorem, the modeled image can be easily obtained by performing the iteration for any starting image of the same size according to D_i and τ_i . The iteration stops while the predetermined tolerance between the original image and modeled image is achieved.

B. Enhancement of Microcalcifications

Based on the above algorithm development, we can enhance microcalcifications by using the fractal modeling approach. Let $f(k, l)$ be the original image, and $g(k, l)$ be the modeled image after n iterations. The procedure is summarized as follows:

Step 1: First, we take the difference operation between $f(k, l)$ and $g(k, l)$:

$$f_1(k, l) = f(k, l) - g(k, l), \quad (k, l) \in N_1 \times N_2, \quad (8)$$

where $f_1(k, l)$ is the residue image.

Step 2: It is appropriate to ignore the negative value of the difference image $f_1(k, l)$, because negative part of $f_1(k, l)$ does not contain any information about spots (including microcalcifications) brighter than the background, so we take

$$f_2(k, l) = \max(0, f_1(k, l)), \quad (k, l) \in N_1 \times N_2, \quad (9)$$

where $f_2(k, l)$ is the enhanced image from which background structures were removed.

Step 3: Image $f_2(k, l)$ contains useful signals and noises. Below a certain threshold T , any signal is considered unreliable. The threshold T is estimated from the image itself as α times the global standard deviation of the noise in an image $f_2(k, l)$. Thus, the value of α is the same for all images, but T depends on each individual image. T can be determined by a two-step estimation process. First the standard deviation of the whole image $f_2(k, l)$ is taken, and the initial threshold T_0 is chosen to be about 2.5 times this global standard deviation. Second, only those pixels in which the gray values are below the initial threshold are used to recalculate the standard deviation of the noise. This is a simplified version of a robust estimation of the standard deviation of noise[10]. The final threshold T is determined by adjusting the value of α so that no subtle cases are missed using human judgement. In our study, we found empirically that $\alpha = 3$ is a suitable choice. The final enhanced image $f_3(k, l)$ is

$$f_3(k, l) = \begin{cases} f_2(k, l), & f_2(k, l) \geq T \\ 0, & f_2(k, l) < T \end{cases} \quad (10)$$

IV. RESULTS AND DISCUSSION

Thirty real mammograms with clustered and single microcalcifications were chosen as testing images. The areas of suspicious microcalcifications were identified by a highly experienced radiologist. The selected mammograms were digitized with an image resolution of $100\mu\text{m} \times 100\mu\text{m}$ per pixel by the laser film digitizer (Model: Lumiscan 150). The image sizes are $1792 \times 2560 \times 12\text{bpp}$. In addition, we generated one simple image based on jigsaw function using computer. The simulated image has a simple periodical texture pattern and has a cluster of spots and a single spot embedded in the simulated background structure. This is a suitable example to test the fractal approach.

A. Evaluation of Enhancement

In order to evaluate the enhancement results of different approaches, we computed the contrast, the background noise level, the peak signal to noise ratio, and the average signal to noise ratio. The definitions of these indexes are

given in the following. The contrast C of an object is defined by [11], [12]

$$C = \frac{f - b}{f + b}, \quad (11)$$

where f is the mean gray-level value of a particular object in the image, called the foreground, and b is the mean gray-level value of a surrounding region called background.

The background noise level can be measured by the standard derivation σ in the background region which is defined as

$$\sigma = \sqrt{\frac{1}{N} \sum_{i=1}^N (b_i - b)^2}, \quad (12)$$

where b_i is the gray-level value of a surrounding background region, and N is the total number of pixels in the surrounding background region.

Since our work focused on specific microcalcification enhancement and the more interesting work for radiologists is to enhance microcalcifications embedded in inhomogeneous and variable background, we defined two new evaluation indexes, the peak signal to noise ratio ($PSNR$) and the average signal to noise ratio ($ASNR$). These definitions were based on the general medical physics measurement and accepted by radiologists for the detection of microcalcifications [13].

The peak signal to noise ratio ($PSNR$) in our work is defined as

$$PSNR = \frac{p - b}{\sigma}, \quad (13)$$

where p is the maximum gray-level value of a foreground.

The average signal to noise ratio ($ASNR$) in our work is defined as

$$ASNR = \frac{f - b}{\sigma}. \quad (14)$$

B. Results and Discussion

We have applied the fractal modeling approach to all real mammograms and the simulated images. Fig. 1 shows the modeled and enhanced results of the simulated image and one of the real mammograms. As we can see in Fig. 1 (b) and (e), the background structure in the simulated image and the general mammographic parenchymal and ductal patterns in mammograms were well modeled. In Fig. 1 (c) and (f), we can see that all small less-structured objects, which include clusters of microcalcifications, single microcalcifications, film defects (such as artifacts caused by scratches on the screen or film emulsion), and sharp edges were clearly enhanced.

In our study, we found that the block size of R_i and pre-determined tolerance δ are two very important parameters

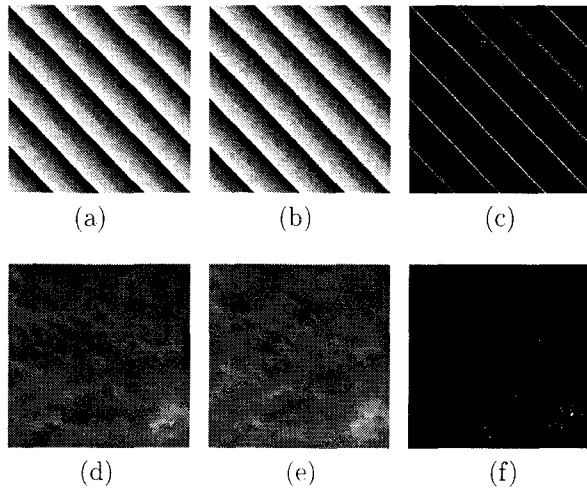


Fig. 1. The modeling and enhancement results of the simulated texture image and one real mammogram using the fractal modeling approach. (a) original image; (b) modeled image; (c) enhanced result; (d) original mammogram; (e) modeled mammogram; (f) enhanced result.

which can affect the modeling process. We have tried different R_i and $\bar{\delta}$ based on all tested images. Fig. 2 shows the curves of the mean square error (MSE) between the original and modeled mammogram with different R_i and $\bar{\delta}$. As we can see in Fig. 2 (a), with fixed $\bar{\delta}$, too large block size would result in visible artificial edge effects on the modeled image, which would increase background noises in the residue image. On the other hand, an R_i of too small size would have less-structured information, therefore making it difficult to search for the correct D_i . A similar situation occurred when we chose $\bar{\delta}$. In Fig. 2 (b), we can see that with fixed R_i , too large $\bar{\delta}$ would introduce more noise and wrong structures on the modeled image. But too small $\bar{\delta}$ would result in no solution of the search process. In our experiment, we found empirically that the suitable block size of R_i is from 32×32 to 8×8 , and the range of $\bar{\delta}$ is from 1.0 to 10.0.

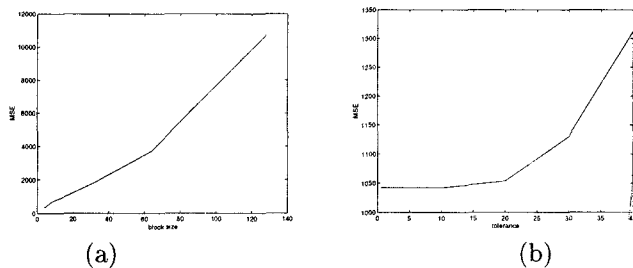


Fig. 2. The effects on the modeled image with different tolerances and block sizes. (a) the plot of MSE between the original and modeled mammogram with different block size R_i , $\bar{\delta} = 10.0$; (b) the plot of MSE between the original and modeled mammogram with different tolerance $\bar{\delta}$, $R_i = 8$.

For the purpose of evaluating the performance of our proposed fractal enhancement method, we chose for comparison two similar enhancement techniques of background removal: the morphological and partial wavelet reconstruction methods [7], [9]. A thresholding was applied to reduce

unreliable noise in the fractal, morphological and wavelet approaches. Fig. 3 shows the enhancement results of clustered and single microcalcifications in the mammograms. The first, second, third, and fourth rows in Fig. 3 correspond to original ROIs, fractal enhancement, wavelet enhancement, and morphological enhancement, respectively. The results indicated that all three approaches removed the background, and in turn enhanced less-structured spots, including microcalcifications. We noted that even for the spots embedded in the bright background (such as dense tissues), the enhancement results were still very promising. Furthermore, we observed that the fractal and morphological approaches can remove more background structures than the wavelet approach does, especially for those ROIs with very low contrast compared with the surrounding background. But the wavelet approach can preserve the overall shape of spots better than the other two approaches.

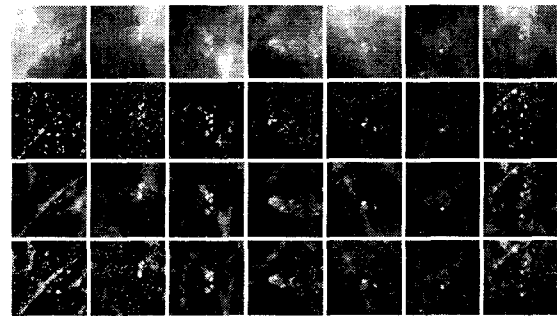


Fig. 3. The enhancement results of clustered microcalcifications on selected ROIs on mammograms using the fractal, wavelet, and morphological approaches.

In order to quantitatively measure the enhancement performance with different approaches, we computed the contrast, the noise level, the peak signal to noise ratio, and the average signal to noise ratio. Table I showed the evaluation results. As we can see from Table I, among these three approaches, the noise level of the fractal approach was the lowest. The contrast, the peak signal to noise ratio, and the average signal to noise ratio of the fractal approach were better than those of the wavelet and morphological approaches. All results obtained in this study are very encouraging, and indicate that the fractal modeling and segmentation method is an effective technique to enhance microcalcifications embedded in inhomogeneous breast tissues.

V. CONCLUSIONS

In this study, we proposed a microcalcification enhancement algorithm based on the fractal modeling scheme. We compared the enhancement results with those based on morphological operations and partial wavelet reconstruction methods. Our study showed that in terms of contrast, peak signal to noise ratio, and average signal to noise ratio, the fractal approach was the best compared to the other methods. The noise level in the fractal approach was also

	original	fractal	wavelet	morphology
σ	141.42	22.90	53.70	40.30
C	0.1918	0.8732	0.7797	0.7960
$PSNR$	4.5971	17.4963	10.3724	11.9312
$ASNR$	1.5473	3.8727	2.6113	3.5766

TABLE I
THE AVERAGES OF EVALUATION RESULTS BASED ON THIRTY
MAMMOGRAMS

lower than the other two methods. These results demonstrated that the fractal modeling method is an effective way to extract mammographic patterns and to enhance microcalcifications. Therefore, the proposed method may facilitate the radiologists' diagnosis of breast cancer.

REFERENCES

- [1] J. G. Elmore, C. K. Wells, C. H. Lee, D. H. Howard, and A. R. Feinstein, "Variability in Radiologists' Interpretations of Mammograms," *The New England Journal of Medicine*, Vol. 331, pp. 1493-1499, 1994.
- [2] F. Lefebvre, H. Benali, R. Gilles, E. Kahn, and R. D. Paola, "A Fractal Approach to the Segmentation of Microcalcification in Digital Mammograms," *Med. Phys.*, Vol. 22, No. 4, pp. 381-390, 1995.
- [3] C. C. Chen, J. S. Daponte, and M. D. Fox, "Fractal Feature Analysis and Classification in Medical Imaging," *IEEE Trans. on Med. Imag.*, Vol. 8, No. 2, pp. 133-142, 1989.
- [4] M. F. Barnsley, *Fractals Everywhere*. New York: Academic Press, 1988.
- [5] A. E. Jacquin, "Image Coding Based on A Fractal Theory of Iterated Contractive Image Transformations," *IEEE Trans. on Images Process.*, Vol. 1, No. 1, pp. 18-30, 1992.
- [6] E. W. Jacobs, Y. Fisher and R. D. Boss, "Image Compression: A Study of The Iterated Transform Method," *Signal Processing*, Vol. 29, No. 3, pp. 251-263, 1992.
- [7] H. Yoshida, K. Doi, and R. M. Nishikawa, "Automated Detection of Clustered Microcalcifications in Digital Mammograms Using Wavelet Transform Techniques," *SPIE Image Processing*, Vol. 2167, pp. 868-886, 1994.
- [8] S. C. Lo, H. P. Chan, J. S. Lin, H. Li, M. T. Freedman, and S. K. Mun, "Artificial Convolution Neural Network for Medical Image Pattern Recognition," *Neural Networks*, Vol. 8, No. 7/8, pp. 1201-1214, 1995.
- [9] J. Dengler, S. Behrens, and J. F. Desaga, "Segmentation of Microcalcifications in Mammograms," *IEEE Trans. on Med. Imaging*, Vol. 12, No. 4, pp. 634-642, December 1993.
- [10] P. J. Huber, *Robust Statistic*. New York: Wiley, 1981.
- [11] W. M. Morrow, R. B. Paranjape, R. M. Rangayyan, and J. E. L. Desautels, "Region-Based Contrast Enhancement of Mammograms," *IEEE Trans. on Medical Imaging*, Vol. 11, No. 3, pp. 392-406, 1992.
- [12] A. F. Laine, S. Schuler, J. Fan, and W. Huda, "Mammographic Feature Enhancement by Multiscale Analysis," *IEEE Trans. on Med. Imaging*, Vol. 13, No. 4, pp. 725-740, December 1994.
- [13] D. P. Chakraborty, "Physical Measures of Image Quality in Mammography," *SPIE Med. Imag.*, Vol. 2708, pp. 179-193, 1996.